



GEOQuébec
2015

Challenges from North to South
Des défis du Nord au Sud

An improved solution for the expansion of cylindrical cavities in Modified Cam Clay.

Vincenzo Silvestri, Youssef Bentaiebi, Mireille Sandrine Ewane et Christian Bravo-Jonard¹

Département des génies civil, géologiques et des mines,
École polytechnique de Montréal, Montréal/Québec, Canada.

Ghassan Abou Samra

Département de génie civil, Université de Moncton/Nouveau-Brunswick, Canada.

ABSTRACT

Recently the authors presented a semi-analytical solution for the undrained plane strain expansion of vertical cylindrical cavities in Modified Cam Clay, in which the hardening parameter p'_c , remained constant. This allowed the determination of explicit expressions for the principal effective stresses. In the present paper, the restriction imposed on p'_c is relaxed, as it varies during undrained shearing in Modified Cam Clay. The new semi-analytical solution is applied to a well-known benchmark case involving remoulded Boston Blue Clay. Comparisons are first made with the case of p'_c constant and then with both a finite difference solution and published finite element results.

RÉSUMÉ

Récemment, les auteurs ont présenté une solution semi-empirique de l'expansion non-drainée et en déformation plane d'une cavité cylindrique dans Cam Clay Modifiée, en gardant constant le paramètre de durcissement p'_c . Ceci a permis de déterminer exactement les contraintes effectives. Dans le présent article, la restriction imposée sur p'_c est relaxée, comme c'est le cas dans Cam Clay Modifié. La nouvelle solution est appliquée à un cas de référence très connu qui implique l'argile bleue de Boston. Des comparaisons sont effectuées avec le cas p'_c constant et aussi avec des solutions aux différences finies et aux éléments finis.

1 INTRODUCTION

Silvestri and Abou-Samra (2012) obtained explicit, closed-form, expressions for the effective stresses generated during the expansion of a vertical cylindrical cavity in Modified Cam Clay (MCC) in plane strain and undrained conditions. The solution was obtained on the assumption that the hardening parameter p'_c , which controls the size of the yield loci, remained constant throughout the expansion. The rationale for the assumption of the constancy of the parameter p'_c was based on preliminary computations which showed that results obtained for $p'_c = \text{constant}$ were quite similar to those found for $p'_c = \text{variable}$, especially for normally consolidated and lightly overconsolidated clays.

In the present technical note, the hardening parameter p'_c of the yield locus varies during the shearing process, as required by the MCC model (See, for example, Wood 2007). New, rigorous, albeit not closed-form, relationships are obtained for the effective stresses. As the MCC model is taken to be applicable in its entirety, although it is known that it applies better to isotropically normally consolidated and lightly overconsolidated clays than to heavily overconsolidated clays, the solution presented herein may serve as a valuable benchmark for verifying various cavity expansion numerical codes based upon the MCC model. Because the determination of the various stress and strain parameters requires the use of simple numerical schemes, without having to resort to sophisticated finite difference and finite elements codes,

the present solution may be considered to follow the steps taken by other investigators, such as Collins and Stimpson (1994), Collins and Yu (1996), Cao et al. (2001), Yu (2000), and Chen and Abousleiman (2012).

The solution obtained in the present technical note is applied for illustration purposes to a benchmark case reported in the literature which involves remoulded Boston Blue Clay. Results are first compared to those obtained by Silvestri and Abou-Samra (2012) for $p'_c = \text{constant}$, and then to finite difference solutions derived using a commercial code. Finally, the results are also compared to published finite element solutions obtained on the same clay.

2 BEHAVIOR OF MODIFIED CAM CLAY IN UNDRAINED COMPRESSION

Before discussing the application of the MCC model to the problem at hand, it should be stressed that the authors are fully aware that this model gives reasonably good results only for isotropically normally consolidated clays. However, because the MCC model is implemented in most commercial numerical codes, the authors chose to retain it even though the approach is applied to clays that were: a) K_0 – consolidated, and b) K_0 – rebounded. Notwithstanding this, it is the intention of the authors to use an anisotropic model in the future. Possible candidates are: a) the anisotropic MCC model (Dafalias 1987; Dafalias et al. 2002, 2006), b) the anisotropic bounding surface plasticity model (Dafalias 1986; Dafalias

and Herrmann 1986; Anandarajah and Dafalias 1986; Ling et al. 2002; Taiebat et al. 2010), and c) the Banerjee model (Banerjee and Yousif 1986; Banerjee et al. 1988). It is believed that both the anisotropic MCC model and the Banerjee model have the advantage that they can account for both inherent and induced anisotropy with relatively few model parameters.

The MCC model remains one of the most employed plasticity model for characterizing the response behaviour of clays incorporating the effect of stress history (Yu 2000; Wood 2007; Chen and Abousleiman 2012). The interested reader may refer to Wood (2007) for a detailed presentation of the model.

Figure 1 presents two undrained compression tests on initially normally consolidated clay specimens (i.e., *ABCDEF* and *CDEF*). The effective stress paths in the $p':q$ plane, where p' is the mean effective stress and q is the deviator stress, are indicated in Fig. 1a. During the tests, the specific volume v ($v = 1 + e$, where e is the void ratio) remains constant (Fig. 1b). Similarly, Fig. 2 presents two undrained compression tests on a heavily overconsolidated clay (i.e., *ABCDEF* and *A'ABCDEF*).

The initial stress state may be either isotropic, as represented by point *A*, or anisotropic, as represented by point *C* on the K_o – consolidation line in Fig. 1a or point *A'* on the K_o – rebound line in Fig. 2a, depending on whether the clay is initially normally consolidated or overconsolidated.

The plastic effective stress path followed by MCC is given by:

$$q = p'_i \left[(M^2 + \eta_i^2) (p'_i / p')^{1/\Lambda} - M^2 \right]^{1/2} \quad [1]$$

where q is the deviator stress and

$q = [(\sigma'_r - \sigma'_\theta)^2 + (\sigma'_\theta - \sigma'_z)^2 + (\sigma'_z - \sigma'_r)^2]^{1/2} / \sqrt{2}$, with $\sigma'_r, \sigma'_\theta, \sigma'_z$ = effective principal radial, tangential, and vertical stresses; p'_i = initial mean effective stress; $\eta_i = q_i / p'_i = 3(1 - K_o) / (1 + 2K_o)$, with q_i = initial deviator stress, and K_o = coefficient of earth pressure at rest; $p' = \text{mean effective stress} = (\sigma'_r + \sigma'_\theta + \sigma'_z) / 3$; $M = q / p'$ at critical state $= 6 \sin \phi' / (3 - \sin \phi')$, with ϕ' = friction angle; $\Lambda = (\lambda - \kappa) / \lambda$, with λ = slope of $v : \ln p'$ curve in loading, κ = slope of $v : \ln p'$ in unloading, and $v = \text{specific volume} = 1 + e$, with e = void ratio (See Figs. 1b and 2b). The yield locus of MCC is given by:

$$q = p' M [(p'_c / p') - 1]^{1/2} \quad [2]$$

where p'_c is the hardening parameter which controls the size of the yield locus, as shown in Figs. 1a and 2a.

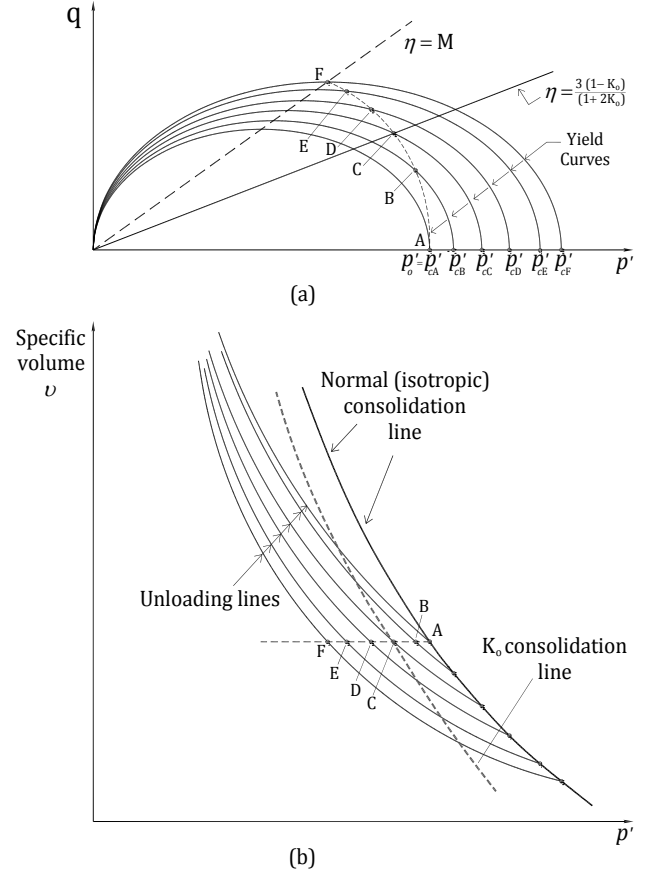


Figure 1. Undrained triaxial compression tests on normally consolidated clay: (a) $p':q$ plane; (b) $v:p'$ plane (adapted from Wood (2007)).

As mentioned above, Silvestri and Abou-Samra (2012) assumed that the hardening parameter p'_c remained constant during shearing. Examination of the curves in Figs. 1a and 2a clearly shows that p'_c varies during the shearing process. The assumption of constant p'_c can be considered to be approximately valid only when the initial stress state, say point *C* in Fig. 1a, is close to the final critical stress state represented by point *F*. This happens only when the soil is lightly overconsolidated (See, for example, Wood 2007).

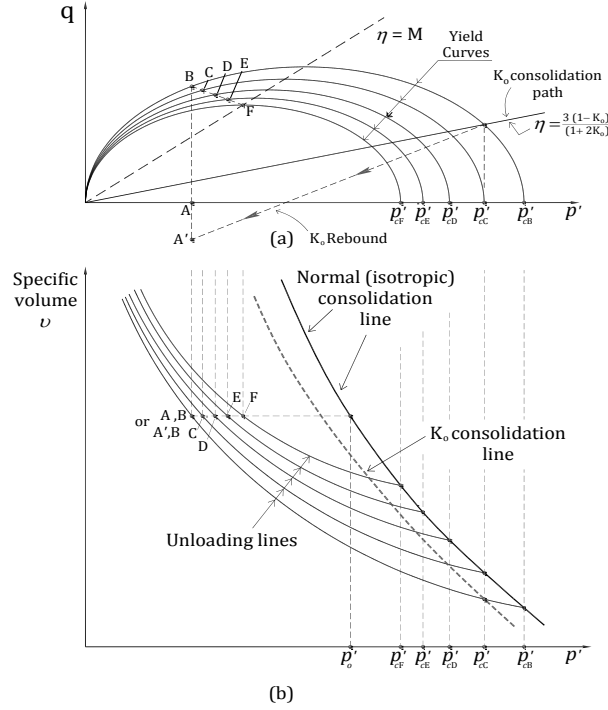


Figure 2. Undrained triaxial compression tests on heavily overconsolidated clay: (a) $p' : q$ plane; (b) $v : p'$ plane (adapted from Wood (2007)).

If the specific volume v of the normally consolidated clay is the same as that of the overconsolidated clay, then the plastic effective stress paths followed by the two specimens in Figs. 1 and 2 are described by the same equation, that is, Eq. 1, provided elastic and plastic strains take place during shearing. The coordinates (p'_f, q_f) at critical state are given by:

$$p'_f = 2^{-\Lambda} p'_o \quad \text{and} \quad q_f = p'_f M = 2^{-\Lambda} M p'_o \quad [3]$$

3 CYLINDRICAL CAVITY EXPANSION IN MODIFIED CAM CLAY

Because the expansion takes place under plane strain in the axial (vertical) direction and in undrained conditions, then

$$d\varepsilon_z = 0 \quad \text{and} \quad d\varepsilon_r = -d\varepsilon_\theta \quad [4]$$

where $\varepsilon_r, \varepsilon_\theta, \varepsilon_z$ are the natural strains in the radial, tangential, and axial directions, respectively. Silvestri and Abou-Samra (2012) showed that the elastic-plastic relationships of MCC are given by:

$$d\sigma'_r = -2G'd\varepsilon_\theta + dp' \left[1 + \frac{6G'\kappa S_r}{vM^2 p'(2p' - p'_c)} \right] \quad [5a]$$

$$d\sigma'_\theta = 2G'd\varepsilon_\theta + dp' \left[1 + \frac{6G'\kappa S_\theta}{vM^2 p'(2p' - p'_c)} \right] \quad [5b]$$

$$d\sigma'_z = dp' \left[1 + \frac{6G'\kappa S_z}{vM^2 p'(2p' - p'_c)} \right] \quad [5c]$$

where G' = shear modulus; and S_r, S_θ, S_z = deviator stresses in the radial, tangential, and axial directions ($S_r = \sigma'_r - p', S_\theta = \sigma'_\theta - p', S_z = \sigma'_z - p'$).

Finite natural strains are considered in both the elastic and plastic phases of expansion (See, also, Yu 2000, and Chen and Abousleiman 2012). Finite strains become approximately equal to small strains in the elastic region, when the strains are relatively small. The shear modulus G' is considered to remain constant during shearing (Zytnski et al. 1978).

The axial stress σ'_z is obtained by integration of Eq. 5c. Because $\sigma'_z - dp' = d(\sigma'_z - p') = dS_z$, Eq. 5c reduces to

$$\frac{dS_z}{S_z} = \frac{6G'\kappa dp'}{vM^2 p'(2p' - p'_c)} \quad [6]$$

Integration of Eq. 6 gives

$$S_z = S_{zi} e^{\frac{6G'\kappa}{vM^2} \int_{p'_i}^{p'} \frac{dp'}{p'(2p' - p'_c)}} \quad [7a]$$

or

$$\sigma'_z - p' = (\sigma'_{zi} - p'_i) e^{\frac{6G'\kappa}{vM^2} \int_{p'_i}^{p'} \frac{dp'}{p'(2p' - p'_c)}} \quad [7b]$$

from which,

$$\sigma'_z = p' + (\sigma'_{zi} - p'_i) e^{\frac{6G'\kappa}{vM^2} \int_{p'_i}^{p'} \frac{dp'}{p'(2p' - p'_c)}} \quad [7c]$$

where S_{zi}, σ'_{zi} , and p'_i are the initial values of S_z, σ'_z , and p' , respectively. The remaining principal stresses σ'_r and σ'_θ are determined by substitution of Eq. 7c into the expressions for p' and q , leading to

$$\sigma'_r = p' - \left(\frac{\sigma'_{zi} - p'_i}{2} \right) e^{\frac{6G'\kappa}{vM^2} \int_{p'_i}^{p'} \frac{dp'}{p'(2p' - p'_c)}} + \tau \quad [8a]$$

and

$$\sigma'_\theta = p' - \left(\frac{\sigma'_{zi} - p'_i}{2} \right) e^{\frac{6G'\kappa}{vM^2} \int_{p'_i}^{p'} \frac{dp'}{p'(2p' - p'_c)}} - \tau \quad [8b]$$

where τ , which is the shear stress in the horizontal plane, is given by

$$\tau = \frac{\sigma'_r - \sigma'_\theta}{2} = \frac{1}{2} \left[\frac{4}{3} q^2 - 3(\sigma'_{zi} - p'_i)^2 e^{\frac{12G'\kappa}{vM^2} \int_{p'_i}^{p'} \frac{dp'}{p'(2p' - p'_c)}} \right]^{1/2} \quad [9]$$

The integrals which appear in Eqs. 7, 8 and 9 must be evaluated numerically because the hardening parameter p'_c varies continuously during the expansion of the cavity. The variation of p'_c is found by equating the plastic volumetric change to the elastic one, that is (See, for example, Wood 2007),

$$v - \lambda \ln \left(\frac{p'_c}{p'_o} \right) = v - \kappa \ln \left(\frac{p'_c}{p'_i} \right) \quad [10]$$

from which,

$$p'_c = p'_i \left(\frac{p'_o}{p'_i} \right)^{1/\Lambda} \quad [11]$$

because the specific volume v remains constant in undrained shearing.

It may be shown that introduction of Eq. 11 into the integrals in Eqs. 7 to 9 leads to incomplete Beta functions (See, for example, Gradshteyn and Ryzhik 1980). However, because either the original integrals or the resulting incomplete Beta functions must be evaluated numerically, the integration in the present study was carried out using the original equations (i.e., Eqs. 7 to 9). The shear strain γ is computed from Eqs. 5a and 5b, leading to

$$\gamma = \frac{\tau}{G'} - \frac{6\kappa}{vM^2} \int_{p'_i}^{p'} \frac{\tau}{p'_i(2p' - p'_o)} dp' \quad [12]$$

where $\gamma = |\varepsilon_r - \varepsilon_\theta| = 2\varepsilon_\theta$, since $\varepsilon_r + \varepsilon_\theta = 0$ in plane strain and undrained shearing. The integral in Eq. 12 must, once again, be evaluated numerically.

Computation of total stresses σ_r , σ_θ , σ_z , and pore pressure u follows the approach of Silvestri and Abou-Samra (2012). As a consequence, their Eqs. 30 to 38b were used in the framework of the present study and are not repeated herein.

It should be mentioned that the shear strain γ in Eq. 12 is also equal to $\ln(r'/r)^2$, where r' and r are generic radial distances of the same material element in the strained and unstrained conditions (See, for example, Yu 2000). In addition, the shear strain γ generated at the wall of the cavity becomes γ_a , that is, $\gamma_a = \ln(a'/a)^2$, where a' and a represent the cavity radii after and before the distortion has occurred. Furthermore, the computation of the limiting radial expansion pressure, which corresponds to $\gamma_a = \infty$, is facilitated by the use of the Almansi tangential strain α which is defined as $\alpha = (r'^2 - r^2)/2r'^2$ and which reduces to $\alpha_o = (a'^2 - a^2)/2a'^2$ at the wall of the cavity (Baguelin et al. 1978).

4 APPLICATION

The theoretical relationships derived previously have been applied to remoulded Boston Blue Clay which is modelled as Modified Cam Clay. The clay properties

which are reported in Table 1 are based on those given by Carter et al. (1979) and Randolph et al. (1979).

Table 1. Initial stress parameters

OCR	K_o	σ'_{zi} [kPa]	$\sigma'_{ri} = \sigma'_{\theta i}$ [kPa]	p'_o [kPa]	p'_c [kPa]	G' [kPa]
1	0.65	300	165	257	270	7570
8	1.35	50.9	68.7	257	365.6	10227

For illustration and comparison purposes, only the normally consolidated (OCR=1) and the overconsolidated clay (OCR=8) cases were retained in the present paper. The Cam Clay parameters are the following: $v = 2.16$, $\lambda = 0.15$, $\kappa = 0.03$, $\Lambda = 0.8$, and $M = 1.2$.

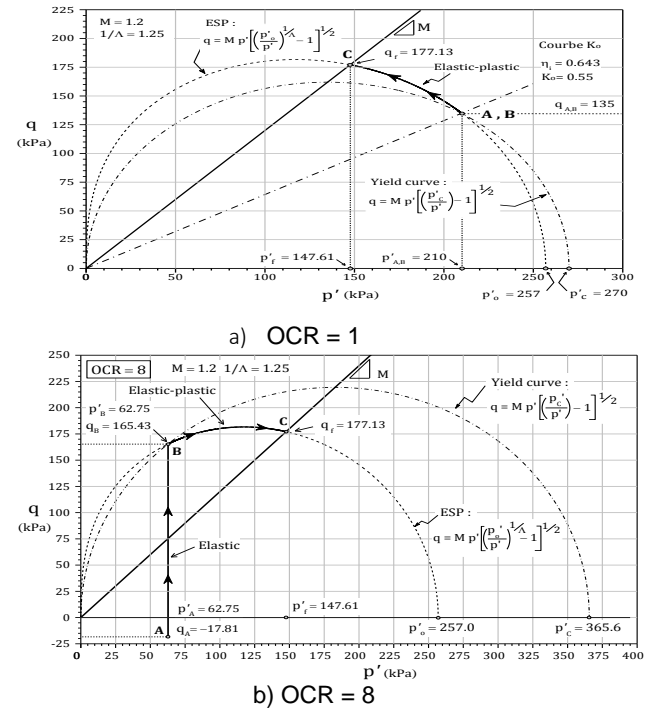
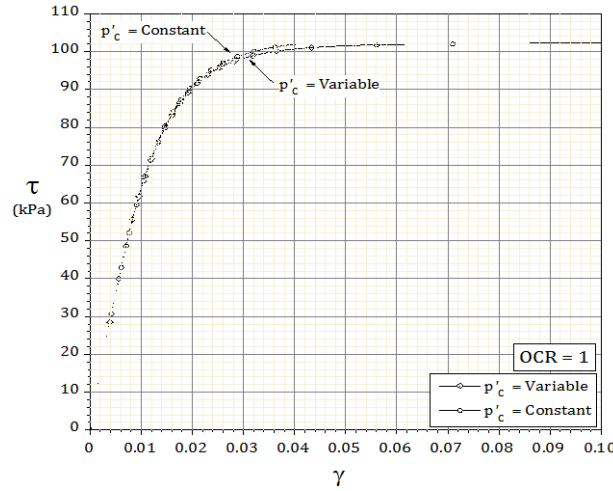


Figure 3. Effective stress paths: (a) OCR = 1; (b) OCR = 8.

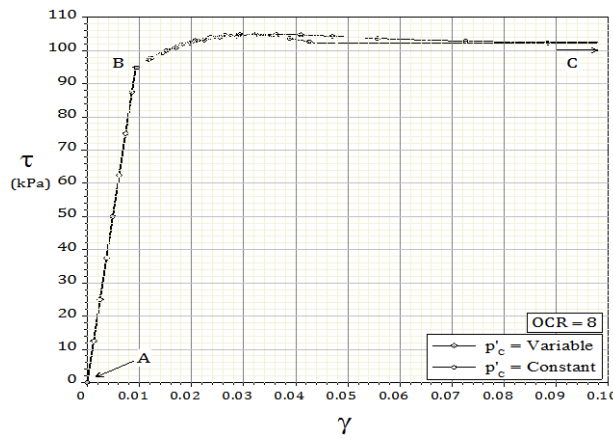
The effective stress paths (ESPs) followed by the two specimens are shown in Fig. 3. The ESP for OCR = 1 in Fig. 3a indicates that the initial stress state, which is represented by point A, is already on the plastic stress path. The critical state is reached at point C ($p'_f = 147.6$ [kPa], $q_f = 177.1$ [kPa]). The ESP for OCR = 8 in Fig. 3b indicates that the path rises vertically until the initial yield curve which corresponds to $p'_c = 365.6$ [kPa] is reached at point B. The clay behaves elastically along AB. Thereafter, the clay becomes plastic and follows the path BC where the critical state is again reached at point C.

The shear stress-shear strain curves were determined by means of Eq. 12 and are presented in Fig. 4. The

curves shown in Fig. 4a for OCR = 1 are quite similar. The curves for OCR = 8 show that the linear elastic phase ends at $\tau = 95.0$ [kPa] where the initial yield curve is reached.



a) OCR = 1



b) OCR = 8

Figure 4. Shear stress-shear strain curves: (a) OCR = 1; (b) OCR = 8.

The similarity between the two curves in Fig. 4b is less perfect than for OCR = 1. At critical state, the shear stress τ is the same for OCR = 1 and OCR = 8. It equals 102.3 [kPa], that is, $\tau = S_u = q_f/\sqrt{3}$. In addition, the effective principal stresses at critical state are given by the following expressions:

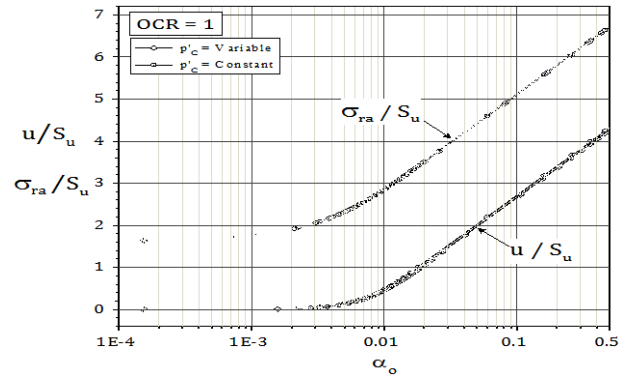
$$\sigma'_{rf} = p'_f + \frac{q_f}{\sqrt{3}} = 147.6 + 102.3 = 249.9 \text{ [kPa]} \quad [13a]$$

$$\sigma'_{zf} = p'_f = 147.6 \text{ [kPa]} \quad [13b]$$

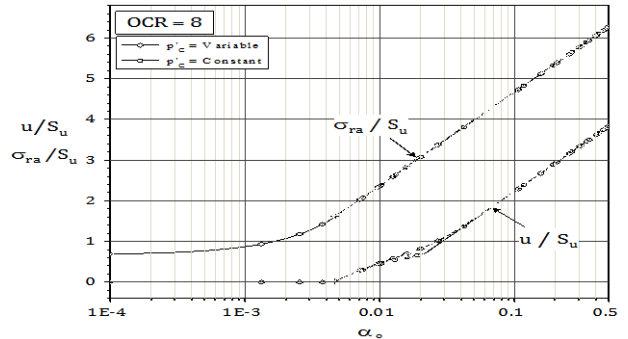
$$\sigma'_{\theta f} = p'_f - \frac{q_f}{\sqrt{3}} = 147.6 - 102.3 = 45.3 \text{ [kPa]} \quad [13c]$$

for both OCR=1 and OCR=8. These values were also found by Carter et al. (1979).

Figure 5 presents the relationships between the total radial stress σ_{ra} and the excess pore pressure u generated at the wall of the cavity as function of the Almansi tangential strain α_o . The limiting values are determined for $\alpha_o = 0.5$ or $\gamma_a = \infty$. While the limiting values of σ_{ra} and u for OCR = 1 are equal to 708.8 [kPa] and 458.9 [kPa], respectively, the corresponding values for OCR = 8 are equal to 647.6 [kPa] and 396.9 [kPa]. Again, the similarity between the two cases (i.e., $p'_c = \text{constant}$ and $p'_c = \text{variable}$) is slightly better for OCR = 1 than for OCR = 8.



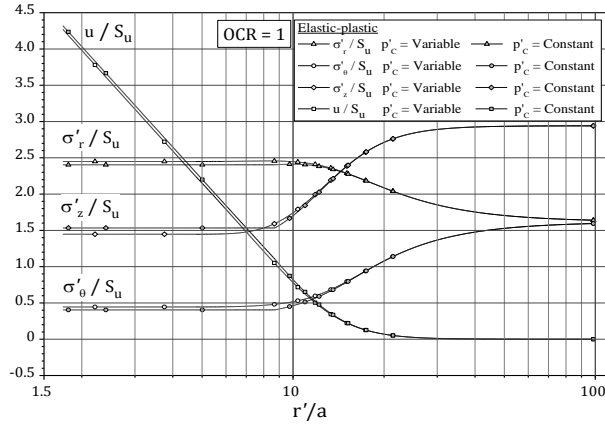
a) OCR = 1



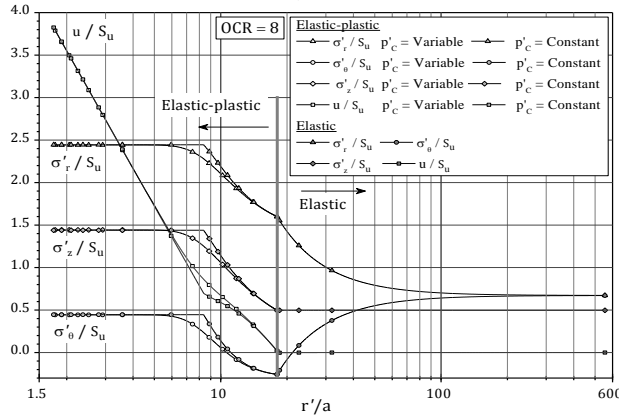
b) OCR = 8

Figure 5. Normalized radial stresses and excess pore pressures generated at wall of cavity: (a) OCR = 1; (b) OCR = 8.

Figure 6 presents the distributions of the effective principal stresses and the pore pressure normalized with respect to $S_u = 102.3$ [kPa] as function of the relative distance r'/a from the center of the cavity, for $a'/a = 2$. Examination of the effective tangential stress relationship for OCR = 8 shows that there exists a tensile region located approximately from $r'/a = 11$ to $r'/a = 21$.



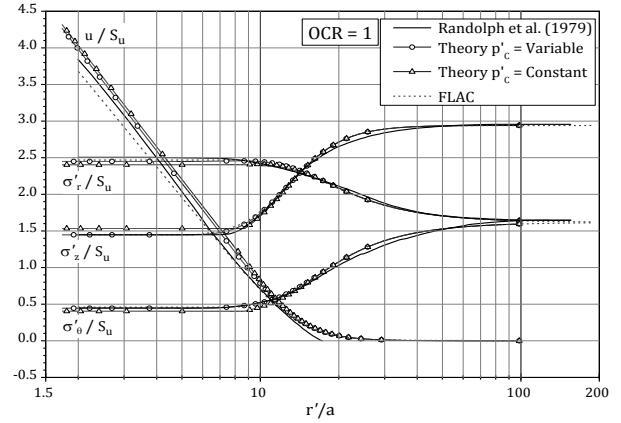
a) OCR = 1



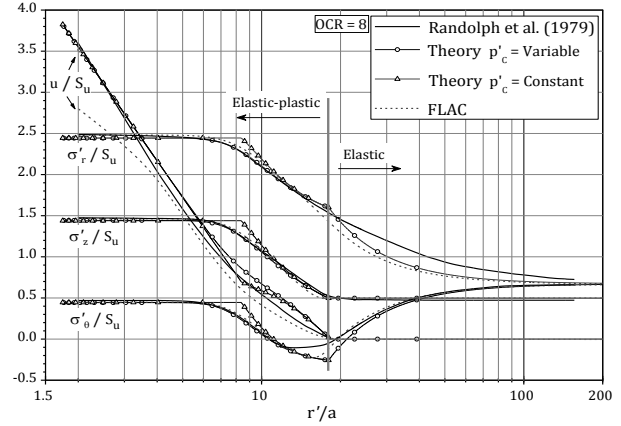
b) OCR = 8

Figure 6. Normalized effective stress and excess pore pressures distributions for $a'/a = 2$: (a) OCR = 1; (b) OCR = 8.

Figure 7 presents for comparison purposes the results reported by Randolph et al. (1979) which were obtained using a finite element analysis. These are compared both with the theoretical results obtained in this study and as well as with numerical results which were determined using the finite difference code FLAC (Itasca 1995). Examination of the various data reported in Fig. 7 shows that the agreement between the numerical methods and the theoretical solution is better for the $p'_c = \text{variable}$ approach than for the $p'_c = \text{constant}$ (simplified) approach.



a) OCR = 1



b) OCR = 8

Figure 7. Comparison between effective stress and excess pore pressure distributions: (a) OCR = 1; (b) OCR = 8.

For completeness, Table 2 presents the values of the total principal stresses as well as the ratio $\sigma_{zf}/(\sigma_{rf} + \sigma_{\theta f})$ at critical state. The theoretical values are compared to those reported by Randolph et al. (1979) which were obtained by means of the finite element analysis mentioned above, for $\alpha_0 = 0.375$ or $\gamma_a = 1.386$, that is, for $a'/a = 2$, where a and a' are, as before, the radii of the cavity, before and after the distortion has occurred. According to Randolph et al. (1979), the stresses would have probably reached their ultimate values for $\alpha_0 = 0.375$, that is, when the cavity radius would have doubled in size. While this is true for the principal effective stresses as shown in Fig. 7, examination of the values reported in Table 2 indicates that the ultimate total stresses were not yet reached when $\alpha_0 = 0.375$.

Table 2: Total principal stresses at critical state

OCR	σ_{zf} [kPa]		σ_{rf} [kPa]		$\sigma_{\theta f}$ [kPa]		$\sigma_{zf}/(\sigma_{rf} + \sigma_{\theta f})$	
	*1	*2	*1	*2	*1	*2	*1	*2
1	606.5	558	708.8	660	504.3	456	0.5	0.5
8	545	528	647.6	631	443	426	0.5	0.5

*1 : This study for $\alpha_o = 0.5$

*2 : Estimated from data reported by Randolph et al. (1979) for $\alpha_o = 0.375$

5 CONCLUSIONS

The following conclusions are drawn on the basis of the theoretical approach presented in this paper:

- Improved principal effective stress relationships are obtained for the plane strain undrained expansion of vertical cylindrical cavities in Modified Cam Clay, by allowing the hardening parameter p'_c to vary during shearing.
- Effective stress paths, stress-strain curves, and stress distributions are obtained for specimens of normally consolidated and overconsolidated remolded Boston Blue Clay, modelled as Modified Cam Clay.
- Comparisons were carried out first with the results obtained by Silvestri and Abou-Samra (2012) by assuming that the hardening parameter p'_c remained constant during shearing. It is shown that while the two approaches (i.e., p'_c = variable and p'_c = constant) yield approximately the same results for OCR = 1, there are nonetheless minor differences for OCR = 8.
- Comparisons with numerical results obtained by means of a finite difference code and with published results derived by means of a finite element solution show good agreement with the present p'_c = variable approach.
- It is also shown by comparing the ultimate total stresses obtained in the present approach with those found from the finite element solution that the final total stress state had not yet been reached when the cavity radius doubled in size.

6 ACKNOWLEDGEMENT

The authors express their gratitude to the Natural Sciences and Engineering Research Council of Canada for the financial support received in this study.

7 REFERENCES

- Anandarajah, A.M., and Dafalias, Y.F. (1986). "Bounding surface plasticity. III: application to anisotropic cohesive soils". *Journal of Engineering Mechanics*, 112(12):1292-1318.
- Baguelin, F., Jézéquel, J.F., and Shields, D.H. (1978). *The pressuremeter and foundation engineering*. Trans Tech Publications, Clausthal, Germany.
- Banerjee, P.K., and Yousif, N.B. (1986). "A plasticity model for the mechanical behavior of anisotropically consolidated clay". *International Journal for Numerical and Analytical Methods in Geomechanics*, 10(5):521-541.
- Banerjee, P.K., Kumbhojkar, A.S., and Yousif, N.B., (1998). "Finite element analysis of the stability of a vertical cut using an anisotropic soil model". *Canadian Geotechnical Journal*, 25(1):119-127.
- Cao, L.F., Teh, C.I., and Chang, M.F. (2001). "Undrained cavity expansion in modified Cam clay". *Géotechnique* 51(4) : 323-334.
- Dafalias, Y.F. (1987). "An anisotropic critical state clay plasticity model". *Proceedings of the Second International Conference on Constitutive Laws for Engineering Materials. Theory and Applications*, January 5-8, Tucson, Arizona, Elsevier, Vol.1, pp.531-521.
- Dafalias, Y.F., and Herrmann, L.R. (1986). "Bounding surface plasticity . II: application to isotropic cohesive soils". *Journal of Engineering Mechanics*, 112(12):1263-1291.
- Dafalias, Y.F., (1986). "Bounding surface plasticity. I: mathematical foundation and hypoplasticity". *Journal of Engineering Mechanics*, 112(9):966-987.
- Dafalias, Y.F., Manzari, M.T., and Akaishi, M.(2002). "A simple anisotropic clay plasticity model". *Mechanics Research Communications*, 29(4):241-245.
- Dafalias, Y.F., Manzari, M.T., and Papadimitriou, A.G. (2006). "SANICLAY:simple anisotropic clay plasticity model". *International Journal for Numerical and Analytical Methods in Geomechanics*, 30(12):1231-1257.
- Collins, L.F., and Stimpson, J.R. (1994). "Similarity solutions for drained and undrained cavity expansions in soils". *Géotechnique* 44(1) : 21-34.
- Collins, L.F., and Yu, H.S. (1996). "Undrained expansions of cavities in critical state soils." *International Journal*

- for Numerical and Analytical Methods in Geomechanics, 20 (7): 489-516.
- Carter, J.P., Randolph, M.F., and Wroth, C.P. (1979). "Stress and pore pressure changes in clay during and after the expansion of a cavity". *International Journal of Numerical and Analytical Methods in Geomechanics*, 3(4): 305-322.
- Chen, S.L., and Abousleiman, Y.N. (2012). "Exact undrained elasto-plastic solution for cylindrical cavity expansion in modified Cam clay". *Géotechnique*, 62(5) : 447-456.
- Gradshteyn, I.S., and Ryzhik, I.M. (1980). *Table of integrals, series and products*. Corrected and enlarged edition. Academic Press, Inc., San Diego, California.
- Ling, H.I., Yue, D., Kaliakin, V.N., and Themelis, N.J.(2002). " Anisotropic bounding surface model for cohesive soils". *Journal of Engineering Mechanics*, 128(7):748-758.
- Randolph, M.F., Carter, J.P. and Wroth, C.P. (1979). " Driven piles in clay-the effect of installation and subsequent consolidation". *Géotechnique*, 24(4) : 361-393.
- Silvestri, V. , and Abou-Samra, G. (2012). "Analytical solution for undrained plane strain expansion of a cavity in modified Cam clay". *Geomechanics and Engineering*, 4(1): 19-37.
- Taiebat, M., Dafalias, Y.F., and Kaynia, A.M. (2010). "Bounding surface model for natural anisotropic clays". *Proceedings of the Ninth HSTAM International Congress on Mechanics, Vardoulakis Mini-Symposia*, July 12-14, Limassol, Cyprus, pp.43-47.
- Wood, D.M. (2007). *Soil behaviour and critical state soil mechanics*. Cambridge University Press, Cambridge.
- Yu, H.S. (2000). *Cavity expansion methods in geomechanics*. Kluwer Academic Publishers, Dordrecht, The Netherlands.
- Zytynski, M., Randolph, M.F., Nova, R., and Wroth,C.P. (1978)."On modelling the unloading-reloading behaviour soils". *International Journal for Numerical and Analytical Methods in Geomechanics*, 2(1) : 87-93.